Four-Way Coupled LES Predictions of Dense Particle-Laden Flows in Horizontal Smooth and Rough Pipes

M. Alletto and M. Breuer

1 Introduction

Turbulent disperse multiphase flows play an important role in many technical applications such as the transport of powders in pneumatic conveying systems. The transport of particles is governed by many physical effects. First of all the continuous flow is in general in the turbulent regime at moderate or high Re. Thus an adequate prediction requires either statistical turbulence models based on RANS or more advanced techniques such as LES. Since in the majority of flows considered complex phenomena such as curved streamlines, secondary flows and transition are involved, the latter is preferred in the present study. The continuous flow provides the basis to determine the fluid dynamic forces such as the drag force and the lift forces due to velocity shear or rotation. Furthermore, the particle motion is strongly influenced by inter-particle collisions. Even for overall dilute two-phase flows, locally high particle concentrations may appear due to the effect of gravity, turbophoresis or the known accumulation of particles in low vorticity regions. These phenomena require to take inter-particle collisions by four-way coupled predictions into account. Last but not least the interaction of the particles with walls plays a dominant role, especially for rough walls. Wall roughness is known to have a significant influence on particle-laden wall-bounded flows. It directly affects the particulate phase due to collisions with rough surfaces and thus needs to be modeled adequately.

In the present contribution all issues mentioned above are incorporated in a four-way coupled Euler-Lagrange LES methodology and applied to the pneumatic conveying of particles through smooth and rough horizontal pipes in the turbulent regime.

M. Alletto · M. Breuer (✉)
Department of Fluid Mechanics, Helmut-Schmidt-Universität Hamburg, Hamburg, Germany
e-mail: breuer@hsu-hh.de

M. Alletto
e-mail: alletto@hsu-hh.de

J. Fröhlich et al. (eds.), *Direct and Large-Eddy Simulation IX*,
ERCOFTAC Series 20, DOI 10.1007/978-3-319-14448-1_76

Two mass loadings (polydisperse) are considered. The secondary flow structures observed in the pipe cross-section are analyzed. The outcome confirms recently published experimental results [2] that the secondary flow is of second kind.

2 Computational Methodology

The continuous phase is simulated in the Eulerian frame of reference using LES. The code is based on a standard 3-D finite-volume method for arbitrary non-orthogonal and block-structured grids. The discretization is of second-order accuracy in space and time. Different subgrid-scale and wall-models can be applied. To take the influence of the particle on the fluid motion into account (two-way coupling), the particle-source-in-cell (PSIC) method is used.

For the particulate phase a huge number of individual particles are tracked throughout the computational domain in a Lagrangian frame of reference taking drag, lift, gravity and buoyancy forces in Newton's second law into account. In order to enable efficient tracking of millions of particles on a block-structured curvilinear grid, the particle tracking is carried out in *c-space* [5] rather than in p-space which possesses the advantage that no search of the particle's new position is required leading to a very fast algorithm.

For tiny particles with a relaxation time of the same order as the smallest fluid time scales the unresolved scales in LES become important for the particle motion. To consider the effect of the subgrid scales, the stochastic model by Pozorski and Apte [8] is applied, where the subgrid-scale kinetic energy is estimated with the help of the scale similarity approach. To account for the rotation of the spherical particles around three Cartesian axes, Newton's second law for the angular momentum is considered.

In contrast to many previous studies relying on statistical particle-particle collision models, in the present investigation a deterministic algorithm is applied for handling the collisions (four-way coupling). The procedure is split into two stages: First, particles are moved based on the equation of motion without inter-particle interactions. Second, the occurrence of collisions during the first stage is examined by a very efficient two-step algorithm [3] for all particles. If a collision is found, the velocities of the collision pair are replaced by the post-collision ones without changing their position. The velocity changes during the collision are predicted by assuming an inelastic collision process of hard spheres including Coulomb's friction leading to either sliding or non-sliding collisions.

The collisions of particles with solid walls is governed by the same relations as long as the wall is ideally smooth. In order to mimic the effect of technically relevant rough walls on the particulate phase, Breuer et al. [4] recently suggested a sandgrain roughness model taking a minimum of measured or empirically determined physical quantities into account. Following Nikuradse's idea a sandgrain roughness model was proposed for the disperse phase in which the wall is covered by a densely packed layer of sand grains idealized by spheres of constant radii. Based on geometric

considerations relying on generally used roughness parameters such as the mean roughness R_z, the local inclination of the wall is determined allowing to predict the inelastic collision of the particle with the rough wall. The sandgrain model also takes the shadow effect into account leading to asymmetric probability density functions of the wall inclination angles, where the mean normal vector is turned towards the incoming particle trajectory [4].

3 Setup and Results

The present applications are concerned with the pneumatic conveying in horizontal pipe flows. Huber and Sommerfeld [6] carried out measurements in 5 m long horizontal glass and steel pipes with a vdiameter $d_{\text{pipe}} = 80\,\text{mm}$. Based on the superficial gas elocity ($U_b = 24\,\text{m/s}$) of the air at standard ambient conditions a Reynolds number of $\text{Re} = U_b\, d_{\text{pipe}}/\nu = 120{,}000$ results. After a certain development length of about $50\, d_{\text{pipe}}$ the flow is assumed to be fully developed. Hence, in the simulations periodic boundary conditions are applied. The computational domain has an extension of $6 d_{\text{pipe}}$ and is discretized by 3×10^7 cells. The wall model of Schumann [9] is applied for the continuous flow.

The particles are spherical glass beads ($\rho_p = 2{,}500\,\text{kg/m}^3$) with a size distribution ranging between about 1.5–98 μm and a number mean diameter of about 40 μm. Experimentally a mass loading of $\eta = 30\,\%$ was investigated [6]. The roughness height for the steel pipe is set to $R_z = 10\,\mu\text{m}$ and the constant describing the surface finishing is given by $C_{\text{Surface}} = 3$ (see Breuer et al. [4]). Two different mass loadings are considered in the simulations: First the statistics computed with a mass loading of $\eta = 30\,\%$ are compared with the experiments of Huber and Sommerfeld [6] to validate the methodology. After that, the origin of the secondary flow observed in the present simulations for both mass loadings η is explained exemplary by means of the computations performed at $\eta = 70\,\%$. Note that a very detailed validation against experiments and DNS and a comprehensive analysis on the appearances of secondary flows in horizontal particle-laden pipe flows can be found in [1].

Figure 1 depicts the simulated mean particle velocity for the glass and the steel pipe compared with the experiments [6]. Obviously, good agreement is found for both cases. Furthermore, it is evident that the wall roughness of the steel pipe leads to a reduction of the influence of the gravitational settling. In case of the glass pipe the mean particle velocity profile shows a strong asymmetry between the lower and upper half of the cross-section due to momentum loss during the wall collisions of the particles settling down at the bottom part of the pipe. Furthermore, the fluid is additionally decelerated at the bottom part due to the highly concentrated particles in this region. Due to the shadow effect in case of the steel pipe the roughness leads to a redistribution of the particle streamwise momentum towards the wall-normal direction. This effect is responsible for a resuspension of the particles and hence to a reduction of the particle concentration in the vicinity of the bottom wall (Fig. 2). This again causes a reduction of the force exerted by the particles on the fluid against the

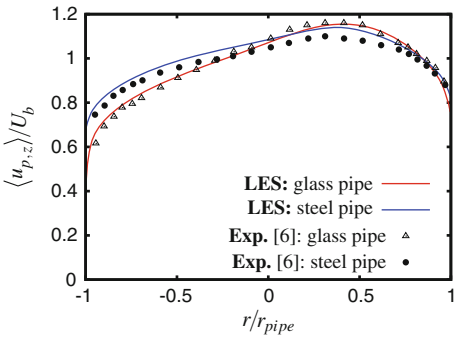

Fig. 1 Mean particle velocity along a *vertical line* for the glass (smooth) and the steel pipe (with roughness)

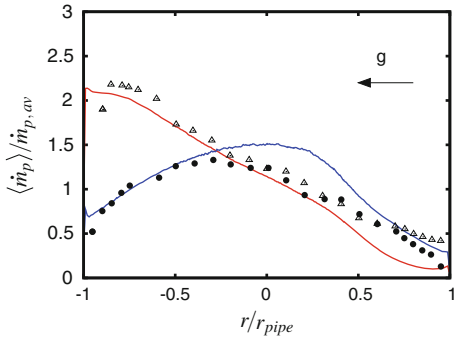

Fig. 2 Mean particle mass flux along a *vertical line* for the glass (smooth) and the steel pipe (with roughness)

mean flow direction in the bottom part of the tube compared with the smooth pipe and hence via the mutual interaction between the particles and the fluid to a higher mean particle velocity near the bottom wall.

Figure 2 shows the mean particle mass flux in streamwise direction at the midplane parallel to the axis of gravity. It is evident that the wall roughness has a drastic effect on this particle statistic. For the smooth wall the particle mass flux near the bottom wall is very high due to the influence of the gravity. For the steel pipe, however, the particles streamwise momentum is redistributed towards the wall-normal direction due to the shadow effect [4, 7]. Hence, after a wall impact the particles acquire a steeper trajectory towards the pipe center since in a pipe the wall-normal vector points towards the pipe center. Consequently, the particles tend to accumulate in this region (focusing effect). Also for the mean particle mass flux good agreement is found between the simulation and the experiment for both cases.

The projected streamlines of the averaged flow field in the pipe cross-section ($\eta = 70\,\%$) are shown in Fig. 3 for the smooth glass pipe and in Fig. 4 for the rough steel pipe. The colormap displays the fluid velocity component against the gravitational acceleration. It is evident that for both cases two rotating cells develop. The fluid flows upstream along the symmetry line. Then it deflects to the left and right in order to circulate downstream along both side walls building a closed vortex. The intensity of the secondary flow in the glass pipe is in the order of 2 % of the

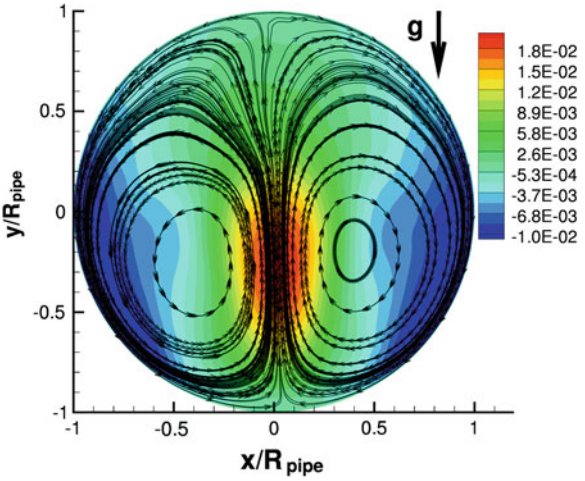

Fig. 3 Projected streamlines for the smooth glass pipe ($\eta = 70\,\%$)

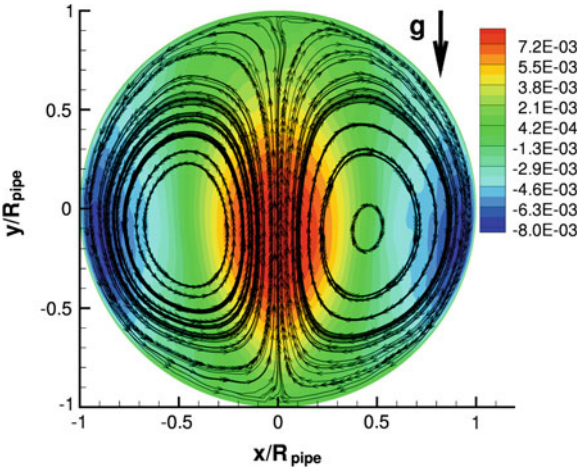

Fig. 4 Projected streamlines for the rough steel pipe ($\eta = 70\,\%$)

bulk velocity and 1 % in the steel pipe. Note that a very similar flow structure can be found in the experiments of Belt et al. [2].

Two reasons for the development of a secondary flow in a circular pipe cross-section can be found [2]: (i) The particles are directly driving the secondary flow via the two-way coupling yielding a secondary flow of first kind or (ii) the particles inhomogeneously attenuate the turbulence leading to an anisotropy in the Reynolds stresses which gives rise to a secondary flow of second kind. In order to exclude that the developing secondary flow is of first kind, the direction and magnitude of the force exerted by the particle on the fluid (time-averaged) is displayed in Fig. 5 for the glass pipe and in Fig. 6 for the steel pipe. The colormap represents the magnitude of the force. It is evident that for both glass and steel pipe the particles decelerate

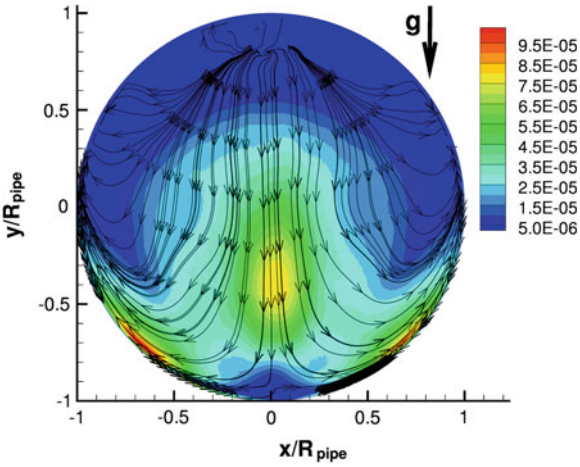

Fig. 5 Mean direction and magnitude of the force exerted by the particles on the fluid, glass pipe ($\eta = 70\,\%$)

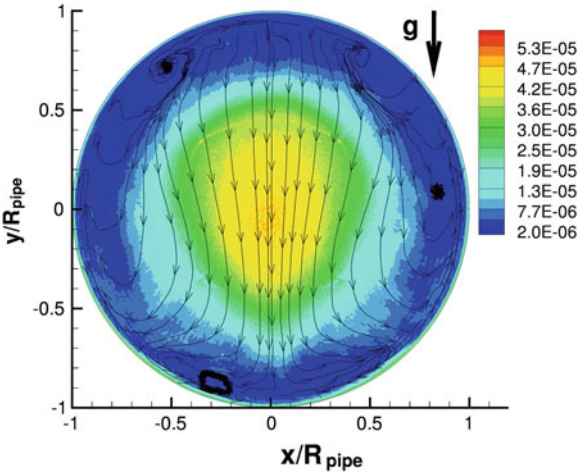

Fig. 6 Mean direction and magnitude of the force exerted by the particles on the fluid, rough steel pipe ($\eta = 70\,\%$)

the fluid in most regions of the pipe cross-section, i.e., the particles are driven by the secondary flow and not the other way round. Hence, the secondary flow of first kind can be excluded.

Following the analysis of Belt et al. [2] and also Alletto and Breuer [1] the gradient of the circumferential Reynolds stress $\langle u'_\theta u'_\theta \rangle$ can be identified as the driving force of the secondary flow. In order to explain the difference in magnitude of the secondary flow between the two investigated pipes, the circumferential Reynolds stress for the glass pipe (Fig. 7) and steel pipe (Fig. 8) is shown. In case of the glass pipe the particles accumulate in the bottom part of the cross-section (concentration contours not shown for the sake of brevity) and hence, the turbulence is more attenuated in this region compared to the top part of the pipe (see Fig. 7). This leads to a gradient of

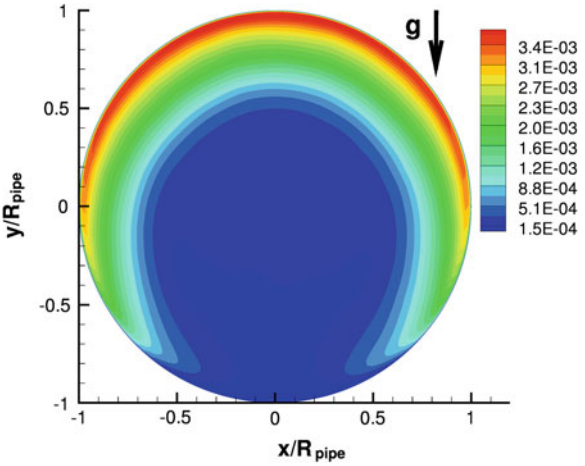

Fig. 7 Mean circumferential Reynolds stress $\langle u'_\theta u'_\theta \rangle$, smooth glass pipe

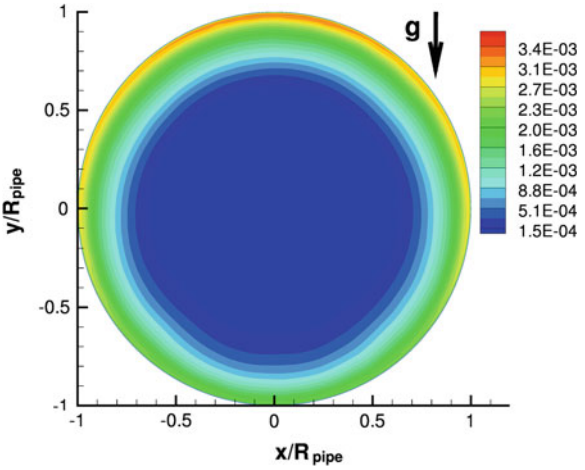

Fig. 8 Mean circumferential Reynolds stress $\langle u'_\theta u'_\theta \rangle$, rough steel pipe

the circumferential Reynolds stress in circumferential direction near the wall which pushes the flow towards the bottom part of the pipe. Due to continuity reasons in the center the fluid flows upwards. The same effect can be found for the steel pipe but not as pronounced as in the glass pipe since the particle are resuspended by the shadow effect and hence accumulate near the pipe center. Nevertheless, turbulence is still more strongly attenuated in the bottom part of the pipe than in the top part leading to a gradient of $\langle u'_\theta u'_\theta \rangle$ in circumferential direction at the wall (Fig. 8) which drives the flow.

4 Conclusions

Secondary flow structures in turbulent flows through horizontal glass and steel pipes were investigated numerically based on a four-way coupled LES. The results were found to be in good agreement with the reference data [6]. Contrary to previous investigations [6, 7] the two-cell secondary flow structure (glass pipe: 2 % U_b; steel pipe: 1 % U_b) is identified to be of the second kind, i.e., driven by the anisotropy of the Reynolds stresses being in line with recently published experimental results [2].

References

1. Alletto, M., Breuer, M.: Prediction of turbulent particle-laden flow in horizontal smooth and rough pipes inducing secondary flow. Int. J. Multiph. Flow **55**, 80–98 (2013)
2. Belt, R.J., Daalmans, A.C.L.M., Portela, L.M.: Experimental study of particle-driven secondary flow in turbulent pipe flows. J. Fluid Mech. **709**, 1–36 (2012)
3. Breuer, M., Alletto, M.: Efficient simulation of particle-laden turbulent flows with high mass loadings using LES. Int. J. Heat Fluid Flow **35**, 2–12 (2012)
4. Breuer, M., Alletto, M., Langfeldt, F.: Sandgrain roughness model for rough walls within Eulerian-Lagrangian predictions of turb. flows. Int. J. Multiph. Flow **43**, 157–175 (2012)
5. Breuer, M., Baytekin, H.T., Matida, E.A.: Prediction of aerosol deposition in 90 degrees bends using LES and an efficient Lagrangian tracking method. J. Aerosol Sci. **37**(11), 1407–1428 (2006)
6. Huber, N., Sommerfeld, M.: Modelling and numerical calculation of dilute-phase pneumatic conveying in pipe systems. Powder Technol. **99**, 90–101 (1998)
7. Lain, S., Sommerfeld, M.: Numerical calculation of pneumatic conveying in horizontal channels and pipes: detailed analysis of conveying behavior. Int. J. Multiph. Flow **39**, 105–120 (2012)
8. Pozorski, J., Apte, S.V.: Filtered particle tracking in isotropic turbulence and stochastic modeling of subgrid-scale dispersion. Int. J. Multiph. Flow **35**, 118–128 (2009)
9. Schumann, U.: Subgrid-scale model for finite difference simulations of turbulent flows in plane channels and annuli. J. Comput. Phys. **18**, 376–404 (1975)